Cost-benefit analysis of coastal flood defence measures in the North Adriatic Sea

Mattia Amadio[1], Arthur H. Essenfelder[1], Stefano Bagli[2], Sepehr Marzi[1], Paolo Mazzoli[2], Jaroslav Mysiak[1], Stephen Roberts[3]

[1] *Centro Euro-Mediterraneo sui Cambiamenti Climatici, Università Ca' Foscari Venezia, Italy*
[2] *Gecosistema, Rimini, Italy*
[3] *The Australian National University, Canberra, Australia*

Correspondence to: Arthur H. Essenfelder (arthur.essenfelder@cmcc.it)

Abstract

The combined effect of extreme sea levels and land subsidence phenomena poses a major threat to coastal settlements. Coastal flooding events are expected to grow in frequency and magnitude, increasing the potential economic losses and costs of adaptation. In Italy, a large share of the population and economic activities are located along the coast of the peninsula, although risk of inundation is not uniformly distributed. The low-lying coastal plain of Northeast Italy is the most sensitive to relative sea level changes. Over the last half a century, the entire north-eastern Italian coast has experienced a significant rise in relative sea level, the main component of which was land subsidence. In the forthcoming decades, climate-induced sea level rise is expected to become the first driver of coastal inundation hazard. We propose an assessment of flood hazard and risk linked with extreme sea level scenarios, both under historical conditions and sea level rise projections at 2050 and 2100. We run a hydrodynamic inundation model on two pilot sites located in the North Adriatic Sea along the Emilia-Romagna coast: Rimini and Cesenatico. Here, we compare alternative risk scenarios accounting for the effect of planned and hypothetical seaside renovation projects against the historical baseline. We apply a flood damage model developed for Italy to estimate the potential economic damage linked to flood scenarios and we calculate the change in expected annual damage according to changes in the relative sea level. Finally, damage reduction benefits are evaluated by means of cost-benefit analysis. Results suggest an overall profitability of the investigated projects over time, with increasing benefits due to increased probability of intense flooding in the next future.

Key-words: coastal inundation Italy extreme sea level rise

Abbreviations: MSL (Mean Sea Level); TWL (Total Water Level); ESL (Extreme Sea Level); SLR (Sea Level Rise); VLM (Vertical Land Movements); DTM (Digital Terrain Model); EAD (Expected Annual Damage)

1. Introduction

Globally, more than 700 million people live in low-lying coastal areas (McGranahan et al. 2007), and about 13% of them are exposed to a 100-year return period flood event (Muis et al. 2016). On average, one million people located in coastal areas are flooded every year (Hinkel et al. 2014). Coastal flood risk shows an increasing trend in many places due to socio-economic growth (Bouwer 2011; Jongman et al. 2012b) and land subsidence (Syvitski et al. 2009; Nicholls and Cazenave 2010), but in the near future sea level rise (SLR) will likely be the most important driver of increased coastal inundation risk (Hallegatte et al. 2013; Hinkel et al. 2014). Evidences show that global sea level has risen at faster rates in the past two centuries compared to the millennial trend (Kemp et al. 2011; Church and White 2011), topping 3.2 mm per year in the last decades mainly due to ocean thermal expansion and glacier melting processes (Mitchum et al. 2010; Meyssignac and Cazenave 2012). According to the IPCC projections, it is very likely that, by the end of the 21st century, the SLR rate will exceed that observed in the period 1971-2010 for all Representative Concentration Pathway (RCP) scenarios (IPCC 2019); yet the local sea level can have a strong regional variability, with some places experiencing significant deviations from the global mean change (Stocker et al. 2013). This is particularly worrisome in regions where changes in the mean sea level (MSL) are more pronounced, considering that even small increases of MSL can drastically change the frequency of extreme sea level (ESL) events, leading up to situations where a 100-year event may occur several times per year by 2100 (Carbognin et al. 2009, 2010; Vousdoukas et al. 2017, 2018; Kirezci et al. 2020). Changes in the frequency of extreme events are likely to make existing coastal protection inadequate in many places, causing a large part of the European coasts to be exposed to flood hazard. Under these premises, coastal floods threaten to trigger devastating impacts on human settlements and activities (Lowe et al. 2001; McInnes et al. 2003; Vousdoukas et al. 2017). In this context, successful coastal risk mitigation and adaptation actions require accurate and detailed information about the characterisation of coastal flood hazard and the performance of alternative coastal defence options. Cost-benefit analysis (CBA) is widely used to evaluate the economic desirability of a disaster risk reduction (DRR) project (Jonkman et al. 2004; Mechler 2016; Price 2018). CBA helps decision-makers in evaluating the efficacy of different adaptation options (Kind 2014; Bos and Zwaneveld 2017).

In this study, we estimate the benefits of coastal renovation projects along the coast of Emilia-Romagna region (Italy) in terms of avoided economic losses from ESL inundation events under both current and future conditions. We select two coastal cities as case study areas: i) Rimini, a touristic hotspot that is currently implementing a seafront renovation project; and ii) Cesenatico, a coastal city that could benefit from similar measures in addition to existing defence mechanisms. We design worst-case scenarios of ESL resulting from the combination of the maximum levels of mean sea level, vertical land movement, storm surge, tide, and wave setup to verify the effectiveness of the above-mentioned coastal defence structures in reducing flood hazard and related impacts over the urban area. To do that, first we employ the 2D-hydrodynamic ANUGA model (Roberts et al. 2015) for simulating coastal inundation associated with ESL scenarios over the two case study areas. The scenarios are calculated by combining probabilistic data from historical ESL events with the estimates of relative mean sea level (RMSL) change for those locations. Each inundation scenario simulated by the hydrodynamic model is evaluated in terms of direct economic impacts over residential areas using a locally-calibrated damage model. The combination of different risk scenarios in a CBA framework allows to evaluate the economic benefits brought by the project implementation in terms of avoided direct flood losses up to the end of the century.

2. Area of study

Located in the central Mediterranean Sea, the Italian peninsula has more than 8,300 km of coasts, hosting around 18% of the country population, numerous towns and cities, industrial plants, commercial harbours and touristic activities, as well as cultural and natural heritage sites. Existing country-scale estimates of SLR impacts up to the end of this century helps to identify the most critically exposed coastal areas of Italy (Lambeck et al. 2011; Bonaduce et al. 2016; Antonioli et al. 2017; Marsico et al. 2017). About 40% of the country's coastal perimeter consist of a flat coastal profile (ISPRA 2012), potentially more vulnerable to the impacts of ESL events. The North Adriatic coastal plain is acknowledged to be the largest and most vulnerable location to extreme coastal events due to the shape, morphology and low bathymetry of the Adriatic sea basin, which cause water level to increase relatively fast during coastal storms (Carbognin et al. 2010; Ciavola and Coco 2017; Perini et al. 2017). The ESL here is driven mainly by astronomical tide, ranging about one meter in the northernmost sector; and meteorological forcing, such as low pressure, seiches and prolonged rotational wind systems, which are the main trigger of storm surge in the Adriatic basin (Vousdoukas et al. 2017; Umgiesser et al. 2020). In addition to that, all the coastal profile of the Padan plain shows relatively fast subsiding rates, partially due to natural phenomena, but in large part linked to human activities (Carbognin et al. 2009; Perini et al. 2017; Meli et al. 2021). As a contributing factor to coastal flood risk, the intensification of urbanization has led to increased exposure along the Adriatic coast during the last 50 years, with many regions building over half of the available land within 300 meters from the shoreline (ISPRA 2012). Figure **1** shows the location of the two case study areas, Cesenatico and Rimini, along with land-cover maps showing the position of coastal defences accounted in this study.

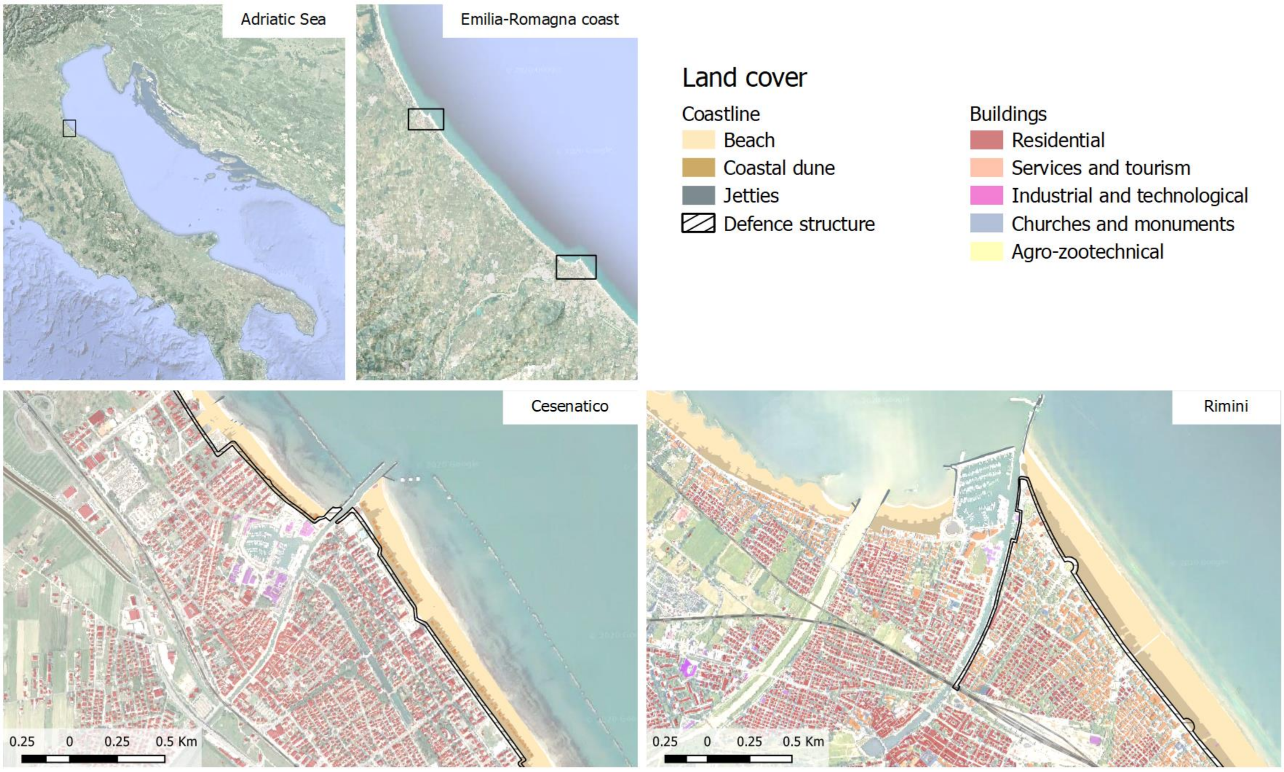

Figure 1. Case-study locations along the Emilia-Romagna coast: Cesenatico and Rimini. The coastal defence structure assessed in this study are shown in black. Buildings' footprint data from Regional Environmental Agency (ARPA) 2020. Basemap © Google Maps 2020.

The number of ESL events reported to cause impacts along the Emilia-Romagna coast shows a steady increase since the second half of the past century (Perini et al. 2011), which is in part explained by to the socio-economic development of the coast exposing increasing asset to flood risk. The landscape along the 130 km regional coastline is almost flat, the only relief being old beach ridges, artificial embankments and a small number of dunes. The coastal perimeter is delineated by a wide sandy beach that is generally protected by offshore breakwaters, groins and jetties. The land elevation is often close to (or even below) the MSL, while the coastal corridor is heavily urbanised. Cesenatico has about 26,000 residents, while Rimini has 150,000. The towns have a strong touristic vocation, hosting large beach resort and bathing facilities along the beach and hundreds of hotels and rental housing located just behind the seaside. Both places have been affected by coastal storms resulting in flooding of buildings and activities, beach erosion and regression of the coastline. The most recent inundation events were observed in March 2010, November 2012 and February 2015. The 2015 event was one of the most severe ever recorded, with ESL values corresponding to a probability of once in 100 years. It caused severe damages along the whole regional coast and, in some locations, required the evacuation of people from their houses; many buildings and roads were covered by sand brought by the flood wave; touristic infrastructures near the shore were seriously damaged, and some port channels overflowed the surrounding areas. The economic impact of the event was estimated topping 7.5 M Eur (Perini et al. 2015).

3. Methodology

3.1 Components of the analysis

Coastal inundation is caused by an increase of total water level (TWL), most often associated to extreme sea level (ESL) events, which are often generated by a combination of high astronomical tide and meteorological drivers such as storm surge and wind waves (Figure **2**). Estimates of ESL are obtained for the North Adriatic up to year 2100 by combining reference hazard scenarios derived from historical records with regionalised projections of SLR (Vousdoukas et al. 2017) and local vertical land movements (VLM) rates (Carbognin et al. 2009; Perini et al. 2017). Four ESL frequency scenarios, namely once in 1, 10, 100 and 250 years, are considered. The hydrodynamic model ANUGA is applied to simulate the inundation of land areas during ESL accounting for individual components (storm surge, tides and waves). Land morphology and exposure of coastal settlements are described by high-resolution DTM and bathymetry, in combination with land use and buildings footprints. The effect of hazard mitigation structures (both designed and under construction) are explicitly accounted in the "defended" simulation scenario, in contrast to the baseline scenario, where only existing defence structures (groins, jetties, breakwaters and sand dunes) are accounted.

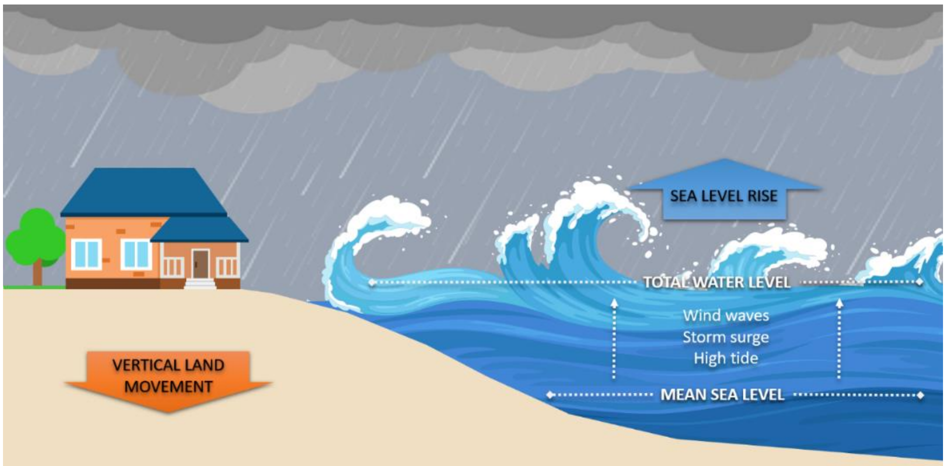

Figure 2. Components of the analysis for extreme sea level events: total water level is the sum of maximum tide, storm surge and wind waves over mean sea level. Vertical land movement and sea level rise affects the mean sea level on the long run.

3.2 Vertical Land Movement

Vertical land movements result from a combination of slow geological processes such as tectonic activity and glacial isostatic adjustment (Peltier 2004; Peltier et al. 2015), and medium-term phenomena, such as sediment loading and soil compaction (Carminati and Martinelli 2002; Lambeck and Purcell 2005). The latter can greatly oversize geological processes at local scale (Wöppelmann and Marcos 2012); in particular, faster subsidence occurs in presence of intense anthropogenic activities such as water withdrawal and natural gas extraction (Teatini et al. 2006; Polcari et al. 2018). Most of the peninsula shows a slow subsiding trend, although with some local variability. An estimate of VLM rates due to tectonic activity has been derived from studies conducted in Italy (Lambeck et al. 2011; Antonioli et al. 2017; Marsico et al. 2017; Solari et al. 2018). The North Adriatic coastal plain shows the most intense long-term geological subsidence rates (about 1 mm per year), increasing North to South. Yet in the last decades these rates were often greatly exceeded by ground compaction rates observed by multi-temporal SAR Interferometry (Gambolati et al. 1998; Antonioli et al. 2017; Polcari et al. 2018; Solari et al. 2018). Observed subsidence is about one order of magnitude faster where the aquifer system has been extensively exploited for agricultural, industrial and civil use since the post-war industrial boom. From the 1970s, however, with the halt of groundwater withdrawals, anthropogenic drivers of subsidence has been strongly reduced or stopped (Carbognin et al. 2009). Nonetheless, subsidence still continues at much faster rates than expected from natural phenomena (Teatini et al. 2005). Geodetic surveys carried out from 1953 to 2003 along the Ravenna coast provide evidence of a cumulative land subsidence exceeding 1 m at some sites due to gas extraction activities. Average subsidence rates observed for 2006-2011 along the Emilia-Romagna coast are around 5 mm/yr, exceeding 10 mm/yr in the back shore of the Cesenatico and Rimini areas and topping 20-50 mm/yr in Ravenna (Carbognin et al. 2009; Perini et al. 2017). Based on these current rates, we assume an average fixed annual VLM of 5 mm in both Cesenatico and Rimini up to the end of the century. This remarkable difference between natural VLM rates and observations would produce a dramatic effect on the estimated SLR scenarios: at present rates, Rimini would see an increase of MSL by 0.15 m in 2050 and more than 0.4 m in 2100 independently from eustatic SLR. Since these rates are connected with human activity, it is not possible to foresee exactly how they will change in the long term.

3.3 Sea Level Rise

The long availability of tide gauge data along the North Adriatic coast allows to assess the changes in MSL during the last century, estimated to be +1.3 mm/year (Scarascia and Lionello 2013). This is consistent with published values for the Mediterranean Sea (Tsimplis and Rixen 2002; Tsimplis et al. 2008) and the Adriatic Sea (Carbognin et al. 2009; Tsimplis et al. 2012). The projections of future MSL account for sea thermal expansions from four global circulation models, estimated contributions from ice-sheets and glaciers (Hinkel et al. 2014) and long-term subsidence projections (Peltier 2004). The ensemble mean is chosen to represent each RCP for different time slices. The increase in the central Mediterranean basin is projected to be approximately 0.2 m by 2050 and between 0.5 and 0.7 m by 2100, compared to historical mean (1970-2004) (Vousdoukas et al. 2017). As agreed with stakeholders, our analysis considers the intermediate emission scenario RCP 4.5, projecting an increase in MSL of 0.53 m at 2100. It must be noted that these projections, although downscaled for the Adriatic basin, do not account for the peculiar continental characteristics of the shallow northern Adriatic sector, where the hydrodynamics and oceanographic parameters partially depend on the freshwater inflow (Zanchettin et al. 2007).

3.4 Tides and meteorological forcing

Storm surge and wind waves represent the largest contribution to TWL during an ESL event. An estimation of these components is obtained for the two coastal sites from the analysis of tide gauge and buoy records, and from the description of historical extreme events presented in local studies (Perini et al. 2011, 2012, 2017; Masina et al. 2015; Armaroli and Duo 2018). This area is microtidal: the mean neap tidal range is 30–40 cm, and the mean spring tidal range is 80–90 cm. Most storms have a duration of less than 24 h and a maximum significant wave height of about 2.5 m. During extreme cyclonic events, the sequence of SE wind (*Sirocco*) piling the water North and E-NE wind (*Bora*) pushing waves towards the coast can generate severe inundation events, with significant wave height ranging 3.3 – 4.7 m and exceptionally exceeding 5.5 m (Armaroli et al. 2012). Fifty significant events have been recorded from 1946 to 2010 on the ER coast, with half of them causing severe impacts along the whole coast and 10 of them being associated with important flooding events (Perini et al. 2017). The most severe events are found when strong winds blow during exceptional tide peaks, most often happening in late autumn and winter. The event of November 1966 represents the highest ESL on records, causing significant impacts along the regional coast: the recorded water level was 1.20 m above MSL, and wave heights offshore were estimated around 6–7 m (Perini et al. 2011; Garnier et al. 2018). The whole coastline suffered from erosion and inundation, especially in the province of Rimini. Atmospheric forcing shown significant variability for the period 1960 onwards (Tsimplis et al. 2012), but there is no strong evidence supporting a significant change in marine storminess frequency or severity for the near future (Lionello 2012;

Lionello et al. 2017, 2020; Zanchettin et al. 2020). Thus, in our model we assume meteorological forcing to remain the same up to 2100.

3.5 Terrain morphology and coastal defence structures

Reliable bathymetries and topography are required in order to run the hydrodynamic modelling at the local scale. Bathymetric data for the Mediterranean Sea were obtained from the European Marine Observation and Data Network (EMODnet) at 100 m resolution. The description of terrain morphology comes from the official high-resolution LIDAR DTM (MATTM, 2019). First, we combined the coastal dataset (2 m resolution and vertical accuracy of ± 0.2 m), and the inland dataset (1 m resolution and vertical accuracy ± 0.1 m) into one seamless layer. Then, the DTM is supplemented with geometries of existing coastal protection elements such as jetties, groins and breakwaters obtained from the digital Regional Technical Map. In Rimini, the *Parco del Mare* (Figure **3**) is an urban renovation project which aims to improve the seafront promenade: the existing road and parking lots are converted into an urban green infrastructure consisting of a concrete barrier covered by vegetated sandy dunes with walking paths. This project also acts as a coastal defence system during extreme sea level events. The barrier rises 2.8 meters along the southern section of the town, south of the marina; no barrier is planned on the northern coastal perimeter. The *Parco del Mare* project is currently under construction and has been taken in account in the evaluation of the "defended" scenarios by adding the barrier to the DTM.

Figure 3. Prototype design of Parco del Mare project in Rimini. Adapted from JDS Architects.

In Cesenatico, the existing defence structures include a moving barrier system (*Porte Vinciane*) located on the port channel, coupled with a dewatering pump which discharge the meteoric waters in the sea. The barriers close automatically if the TWL surpasses 1 meter over the mean sea level, preventing floods in the historical centre up to 2.2 meters of TWL. Additional defence structures include the winter dunes, which consist of a 2.2 meter-tall intermittent, non-reinforced sand barrier. In the defended scenario, we envisage a coastal defence structure similar to Rimini's *Parco del Mare* project, spanning both North and South of the port channel with a total length of 7.8 km. A proper setup of the inundation model required to first perform some manual editing of the DTM using additional reference data (i.e. on-site observations or aerial photography) in order to produce an elevation model that realistically represent the land morphology and associated water dynamics (e.g. removal of non-existent sink holes). Bridges and tunnels are the most critical elements that required DTM correction in order to avoid misrepresentations of the water flow routing.

3.6 Inundation modelling

In this study we use ANUGA, a 2D hydrodynamic model suitable for the simulation of flooding events resulting from riverine peak flows and storm surges (Roberts 2020). Being a 2D hydrodynamic model, ANUGA does not resolve vertical convection, waves breaking or 3D turbulence (e.g. vorticity), thus it not accounting for the swash component of wave runup. The fluid dynamics in ANUGA is based on a finite-volume method for solving the shallow water wave equations, thus being based on continuity and simplified momentum equation. The model includes also an operator module that simulates the removal of sand associated with over-topping of a sand dune by sea waves, which is applied to explore scenarios where a sand dune barrier provides protection for the land behind. The operator simulates the erosion, collapse, fluidisation and removal of sand from the dune system (Kain et al. 2020); the dune erosion mechanism relies on a relationship based on Froehlich (2002). This option is enabled only in the undefended scenario for Cesenatico, where non-reinforced sand dunes are prone to erosion.

The case study areas are represented by an irregular triangular mesh in which water level, water depth and horizontal momentum are computed. The size of the triangles is variable within the mesh, thus allowing or a better representation in regions of particular interest, such as along the coastline, in urban areas, and inside the canals. Six different regions are used in each case study to define different triangular mesh resolution, varying from higher resolution areas of 16 m² for canals and coastal defence structures, to lower resolution of 900 m² for sea areas. Figure **4** presents the considered regions and the respective resolutions for the case study cities. The resulting irregular mesh counts with 636,938 triangles for the Cesenatico case study, and 1,198,604 triangles for the Rimini case study.

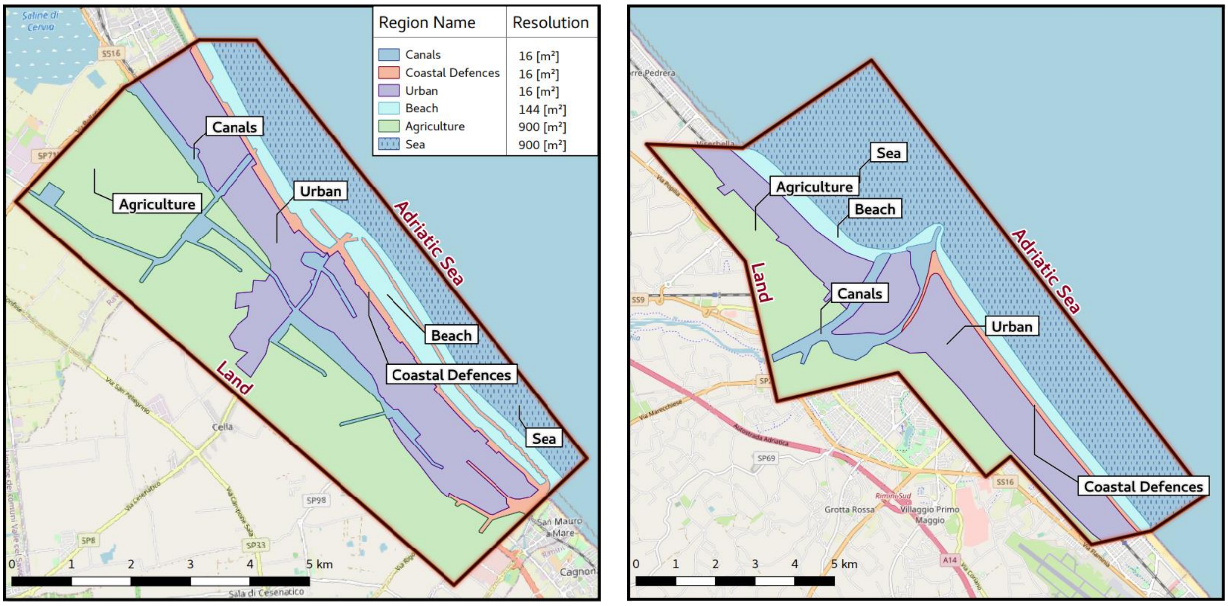

Figure 4. The definition of simulation domain for the cities of Cesenatico (left) and Rimini (right).

Boundary conditions are used to specify the water level dynamics (i.e. forcing term) along the Adriatic Sea margin of each case study area in ANUGA's domain. Based on these conditions, the model computes the total water level insisting on the coast, the resulting water depth of inundation, and the horizontal momentum on an irregular triangular grid s. Figure **5** shows how boundary conditions are set-up in ANUGA during a theoretical storm tide event for an example case of a once-in-10 years return period (additional setups for other RPs can be found in Annex 1). Each of the components shown is considered independently, according to the intensity (i.e. water level) and duration of the respective storm tide event, and added to generate the black continuous line representing the storm tide level (or total water level, TWL) as a boundary condition in ANUGA.

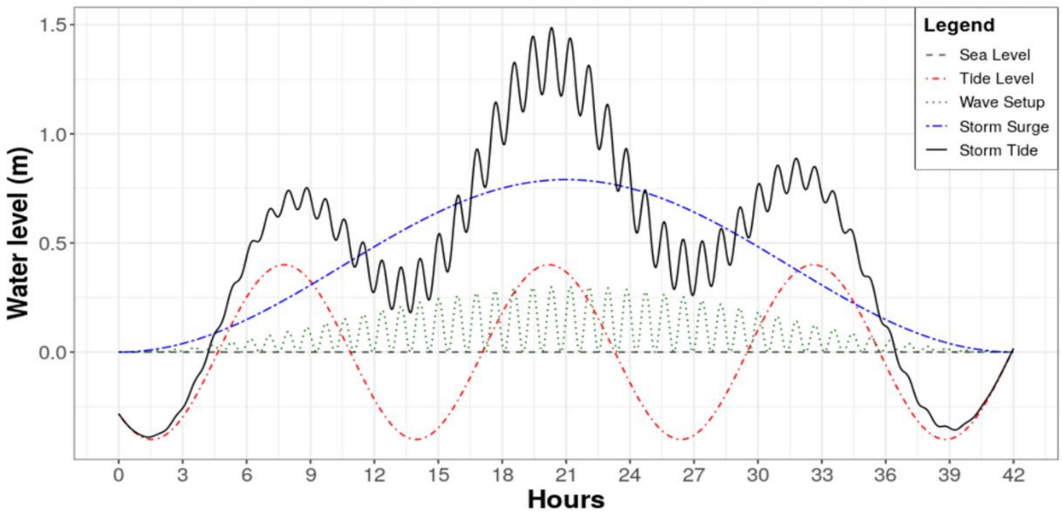

Figure 5. Total Water Level (black) as a sum of tide (red), storm surge (blue) and wave setup (green) for ESL scenario 1 in 10 years. Additional figures for all RPs are found in Annex 1.

In our application, we estimate the TWL on the coastland at every timestep as the sum of extreme values for storm surge level (*SS*), wave setup (*Ws*), and max tide (*Tmax*). Storm surge peak is set to coincide with the tidal peak at the mid of the event, thus producing a maximum TWL value. As considered, our approach is precautionary as it provides worst-case scenario ESL values. The components of TWL are obtained from existing probabilistic analysis of extreme events conducted on the regional coast (Perini et al. 2016, 2017) and later adopted by the Regional Environmental Agency to define the official coastal flood hazard zones (ARPAE 2019). The probability of occurrence for ESL scenarios is expressed in terms of return period (*RP*), which is the estimated average time interval between events of similar intensity, accounting for all variables combined. The high tide contribution grows from 0.40 m to 0.45 m, while wave setup near the shore ranges from 0.22 m to 0.65 m. We select the scenario RP 250 years as the upper boundary of hazard intensity, considering all components of TWL to reach their most extreme values and summing up to +2.5 meters over MSL. Additional details are wave period (*Wp*, in seconds) and event duration (*Time*, in hours), required for the hydrodynamic simulation of coastal flooding events and the determination of the maximum extent of inland water propagation. Both variables are obtained from analysis of observations recorded during historical ESL events on the coast of Emilia-Romagna from 1946 to 2010 (Perini et al. 2011), matched with the probabilistic distribution of RP scenarios (Armaroli et al. 2012; Armaroli and Duo 2018). In our scenarios, wave direction is set to be oriented perpendicular to the coast. Table **1** summarizes the ESL components according to the four probability scenarios. The output of the simulation consists of maps representing flood extent, water depth and momentum at every time step (1 second), projected on the high-resolution DTM grid.

Table 1. components of TWL during an ESL event under historical conditions and projected conditions (2050 and 2100), accounting for both SLR (RCP 4.5) and average VLM rate.

	Extreme event features				**Historical**	**2050**			**2100**		
RP (years)	*SS* (m)	*Tmax* (m)	*Ws* (m)	*Time* (h)	*TWL* (m)	*SLR* (m)	*VLM* (m)	*TWL* (m)	*SLR* (m)	*VLM* (m)	*TWL* (m)
1	0.60	0.40	0.22	32	1.22	0.14	0.19	1.55	0.53	0.44	2.19
10	0.79	0.40	0.30	42	1.49	0.14	0.19	1.82	0.53	0.44	2.46
100	1.02	0.40	0.39	55	1.81	0.14	0.19	2.14	0.53	0.44	2.78
250	1.40	0.45	0.65	75	2.50	0.14	0.19	2.83	0.53	0.44	3.47

ANUGA takes into account the boundary conditions specified in Table 1 and dynamically shown in Figure 5 to simulate the flood dynamics within the domain, such as water flowing through canals and the flooding of land areas. For each return period scenario, a different hypotetical ESL event is designed in order to match the maxima level of tide and surge (following the worst-case scenario assumption, as previously mentioned). These synthetic events are designed assuming trigonometric functional forms describing the oscillation of water level due to the different components defining ESL (Boon 2004; Fuhrmann et al. 2019; Familkhalili et al. 2020). Each component, then, has a different period and magnitude, to reflect specific contributions of each component. Regarding the wave component, since ANUGA is a 2D model that cannot simulate wave breaking and the swash component of wave runup, we simulate just the wave setup component based on values reported in regional studies (Perini et al. 2012, 2016). The wave setup is a relevant component of the total water level by contributing to the flood dynamics due to the momentum of waves, particularly when directed inlands (Melet et al. 2020). We consider wave setup as a function of the intensity of the storm surge level, as shown by the green dashed line in Figure 5. The maximum wave setup level is designed to coincide with the timing of maximum storm tide level, following the assumption of worst-case scenario, while wave direction is aligned with the storm surge direction, thus being perpendicular to the coastline.

3.7 Risk modelling and Expected Annual Damage

Direct damage to physical asset is estimated using a customary flood risk assessment approach originally developed for fluvial inundation, which is adapted to coastal flooding assuming that the dynamic of impact from long-setting floods depends on the same factors, namely: 1) hazard magnitude, and 2) size and value of exposed asset. Indirect economic losses due to secondary effects of damage (e.g. business interruption) are excluded from the computation. Hazard magnitude can be defined by a range of variables, but the most important predictors of damage are water depth and the extension of the flood event (Jongman et al. 2012a; Huizinga et al. 2017). Land cover definitions and buildings footprints help to estimate the exposed capital including residential buildings, commercial and industrial activities, infrastructures, historical and natural sites. The characterization of exposed asset is built from a variety of sources, starting from land use and buildings footprints obtained from the Regional Environmental Agencies geodatabases and the Open Street Map database (Geofabrik GmbH 2018). Additional indicators about buildings characteristics are obtained from the database of the 2011 Italian Census (ISTAT 2011), while mean construction and restoration costs per building types are obtained from cadastral estimates (CRESME 2014). The asset representation is static, thus not accounting for changes in land use nor population density, while allowing for the direct comparison of hazard mitigation options' results. A depth-damage function was previously validated on empirical records (Amadio et al. 2019) and then applied in order to translate each hazard scenario into an estimate of economic risk, measured as a share of total exposed value. The damage function applies only to residential and mixed-residential buildings, the area of which represents about 93% of total exposed footprints; other types (such as harbour infrastructures, industrial, commercial, historical monuments and natural sites) are excluded from risk computation. Abandoned or under-construction buildings are also excluded from the analysis. To avoid overcounting of marginally-affected buildings, we set two threshold conditions for damage calculation: flood extent must be greater than or equal to 10 m^2, and maximum water depth greater than or equal to 10 cm. The damage/probability scenarios are combined together as Expected Annual Damage (EAD). EAD is the damage that would occur in any given year if damages from all flood probabilities were spread out evenly over time; mathematically, EAD is the integration of the flood risk density curve over all probabilities (Olsen et al. 2015), as in equation **1**.

$$EAD = \int_0^1 D(p)\, dp \tag{1}$$

The integration of the curve can be solved either analytically or numerically, depending on the complexity of the damage function *D(p)*. Several different methods for numerical integration exist; we use an approach where EAD is the sum of the product of the fractions of exceedance probabilities by their corresponding damages (Figure **6**). We calculate *D(p)*, which is the damage that occurs at the event with probability *p*, by using the depth-damage function for each hazard scenario. The exceedance probability of each event (*p*) is calculated based on exponential function as shown in equation **2**.

$$p = 1 - e^{\left(\frac{-1}{RP}\right)} \tag{2}$$

Events with a high probability of occurrence and low intensity (below RP 1 year) are not simulated, as they are assumed to not cause significant damage. This is consistent with the historical observations for the case study area, although this assumption could change with increasing MSL.

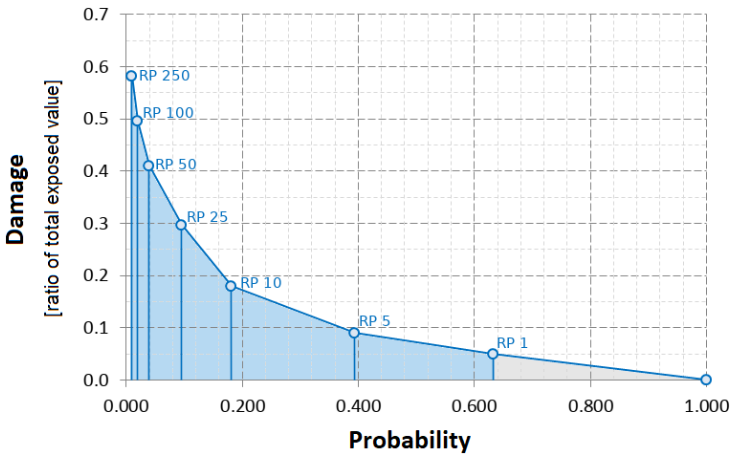

Figure 6. Schematic representation of the numerical integration of the damage function *D(p)* with respect to the exponential probability of the hazard events. Damage (Y axis) represents the ratio of damage to the total exposed value estimated up to the most extreme scenario (RP 250 years). Events with a probability of occurrence higher than once in a year are expected to not cause damage (grey area).

3.8 Cost-Benefit Analysis

A CBA should include a complete assessment of the impacts brought by the implementation of the hazard mitigation option, i.e. direct and indirect, tangible and intangible impacts (Bos and Zwaneveld 2017). The project we are considering, however, has not been primarily designed for DRR purpose: instead, it is meant as an urban renovation project which aims to consolidate the touristic vocation of the area, to improve the quality of life and the urban environment (Comune di Rimini 2018). This implies some large indirect effects on the whole area, most of which are not strictly related to disaster risk management and, overall, very difficult to estimate ex-ante. Our evaluation focuses only on the benefits that are measurable in terms of direct flood losses reduction. Regarding the implementation costs, the CBA accounts for the initial investment required for setting up the adaptation measure, and operational costs through time. According to the *Parco del Mare* project funding documentation (Comune di Rimini 2019a, b, 2020, 2021a, b), the total cost of the project (to be completed during 2021) is 33.3 M Eur, corresponding to 5.55 M Eur per Km of length. No information is available about maintenance costs of the opera, but given the nature of the project (static defense with low structural fragility), we assume they will be rather small compared to the initial investment. Ordinary annual maintenance costs are accounted as 0.1% of the total cost of the project. The same costs are assumed for the hypothetical barrier in Cesenatico, resulting in an initial investment cost of 43.3 M. Costs and benefit occurring in the future periods need to be discounted, as people put higher value on the present (Rose et al., 2007). This is done by adjusting future costs and benefits using an annual discount rate (*r*). We chose a variable rate of *r = 3.5* for the first 50 years and *r = 3* from 2050 onward (Lowe 2008). A sensitivity analysis of discount rate is included in Annex 2. The three main decision criteria used in CBA for project evaluation are the Net Present Value (NPV), the Benefit/Cost Ratio (BCR) and the payback period. The NPV is the sum of Expected Annual Benefits (*B*) up to the end of the time horizon, discounted, minus the total costs for the implementation of the defense measure, which takes into account initial investment plus discounted annual maintenance costs (*C*). In other words, the NPV of a project equals the present value of the net benefits ($NB_i = B_i - C_i$) over a period of time (Boardman et al. 2018), as in equation **3**:

$$NPV = \mathrm{PV(B)} - \mathrm{PV(C)} = \sum_{t=0}^{n} \frac{NB_r}{(1+r)^t} \tag{3}$$

Positive NPV means that the project is economically profitable. The BCR is instead the ratio between the benefits and the costs; a BCR larger than 1 means that the benefits of the project exceed the costs on the long term and the project is considered profitable. The payback period is the number of years required for the discounted benefits to equal the total costs.

4. Results

4.1 Inundation scenarios

Once the setup is completed, the hydrodynamic model performs relatively fast: each simulation is carried at half speed compared to real time, requiring about 24 hours to simulate a 12 h event. Parallel simulations for the same area can run on a multicore processor, improving the efficiency of the process. The output of the hydrodynamic model consists of a set of inundation simulations that include several hazard intensity variables in relation to flood extent: water depth, flow velocity, and duration of submersion. ESL scenarios are then summarized into static maps, each one representing the maximum value reached by hazard intensity variables during the simulated event at about 1 meter resolution. The flood extents corresponding to each RP scenario are shown for Rimini (Figure **7**) and Cesenatico (Figure **8**).

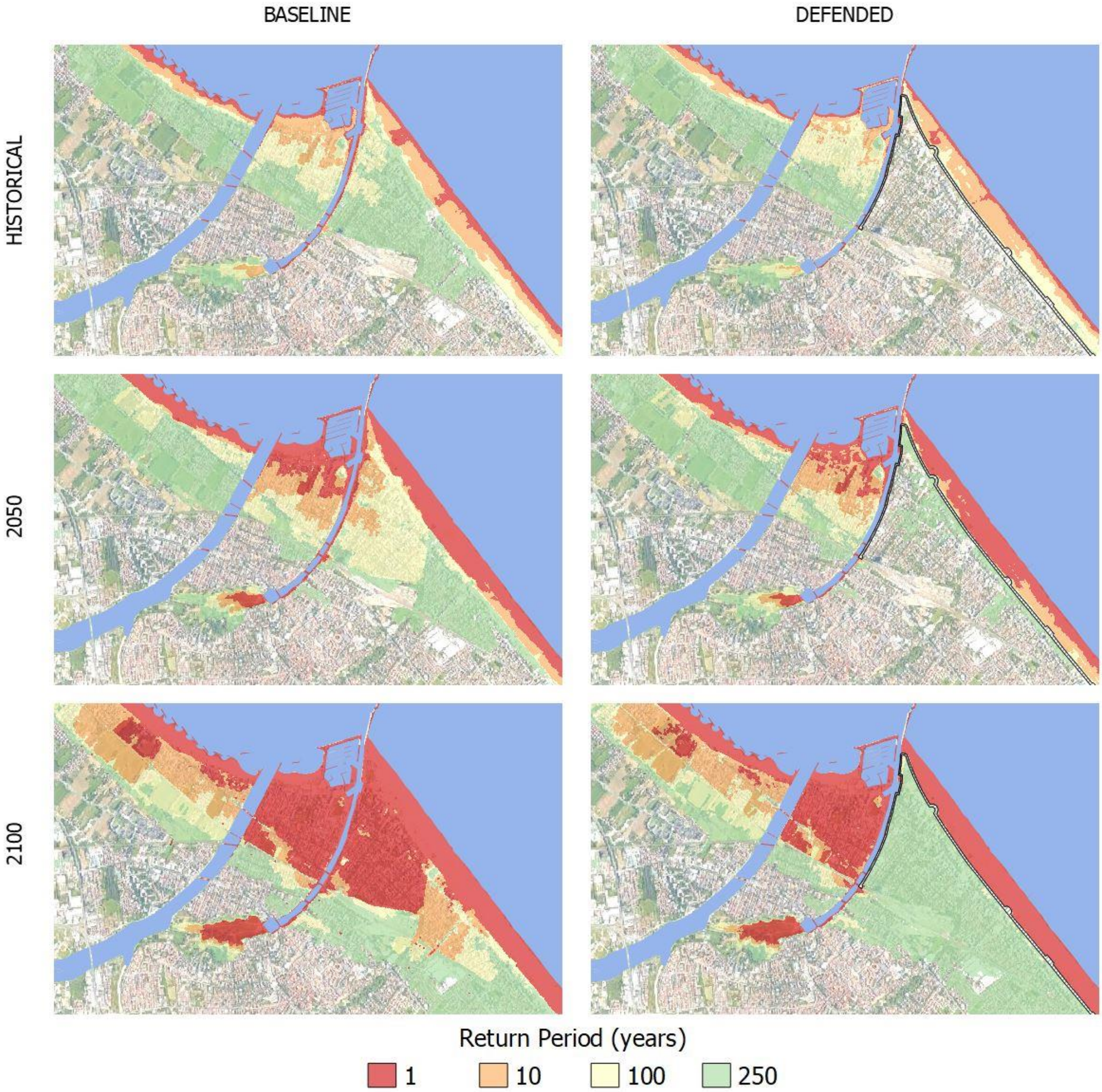

Figure 7. Rimini, extent of land affected by flood according to frequency of occurrence of ESL event up to 2100 for the baseline [left] and the defended scenario [right]. Basemap © Google Maps 2020.

In Rimini, the *Parco del Mare* barrier produces benefits in terms of avoided damage in the south-eastern part of the town (high-density area) for ESL events with a return period of 100 years or less. The north-western part and the marina are outside of the defended area; these areas are therefore subject to a similar amount of flooding across scenarios. In all the simulations, the buildings located behind the marina are the firsts to be flooded. In fact, the new and the old port channels located on both sides of the marina represent a hazard hotspot: as shown in the maps, the failure of the eastern channel, which has a relatively low elevation, is likely to cause the water to flood the eastern part of the town, even during inundation events that would not surpass the beach. In the defended scenarios, where both the coastal and the canal barriers are enabled, the flood extent in the south-eastern urban area becomes almost zero for ESL events with a probability of once in 100 years, even when accounting for SLR up to 2100. Under the most exceptional ESL conditions (RP 250 in 2100), the barrier is overtopped, generating a flood extent similar to the baseline scenario for the same occurrence probability.

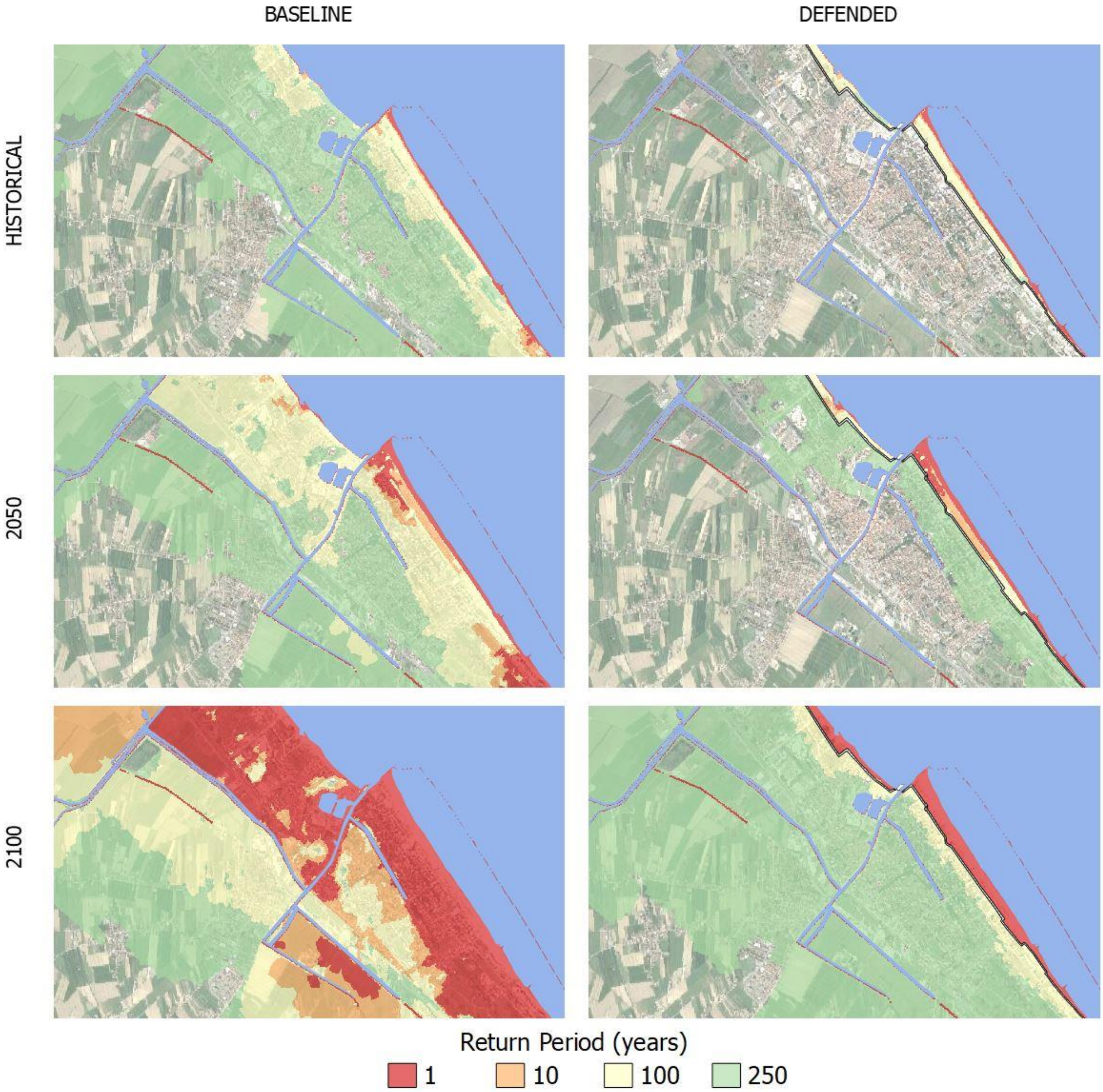

Figure 8. Cesenatico, extent of land affected by flood according to frequency of occurrence of ESL event up to 2100 for the baseline [left] and the defended scenario [right]. Basemap © Google Maps 2020.

In Cesenatico, a barrier designed similarly to *Parco del Mare* could provide significant reduction of flood extents under most hazard scenarios. Its effectiveness would be greater than in Rimini thanks to the complementary movable barrier system in use, which seals the port channel allowing to wall off the whole coastal perimeter, reducing the chance of water ingression in the urban area. In contrast, the erodible winter dune in the baseline defense scenario can only hold the heavy sea for shorter, less intense ESL events (RP 1 – 10 years), and becomes ineffective with more exceptional, long-lasting events; from 2050 on, the winter dune could be surmounted and dismantled by sea waves even during frequent events (RP 1 year).

4.2 Expected Annual Damage

The Expected Annual Damage is calculated as a function of maximum exposed value and water depth. In Rimini, the EAD grows from around 650 thousand Eur under historical conditions to 2.8 million Eur in 2050 and more than 32.3 million Eur in 2100. Under less severe ESL scenarios (RP below 100 years), the risk remains mostly confined around the marina, which is located outside the defended area, producing an expected damage below 10 thousand Eur. Under more extreme ESL scenarios, the benefits of the *Parco del Mare* project protecting the southern part of Rimini become more evident, avoiding about 65% of the expected damages in the defended scenarios compared to the undefended ones. The damage avoided in the defended scenarios grow almost linearly with the increase of the baseline EAD under future projections of sea level rise: under the defended scenario, the EAD is reduced on average by 45% in comparison with the undefended scenario (Figure **9**, left). The project produces benefit up to scenario RP 250 years in 2100, where a projected TWL of 3.5 meters would cause the overtopping of the barrier, reducing the benefits to almost zero (Figure **9**, right).

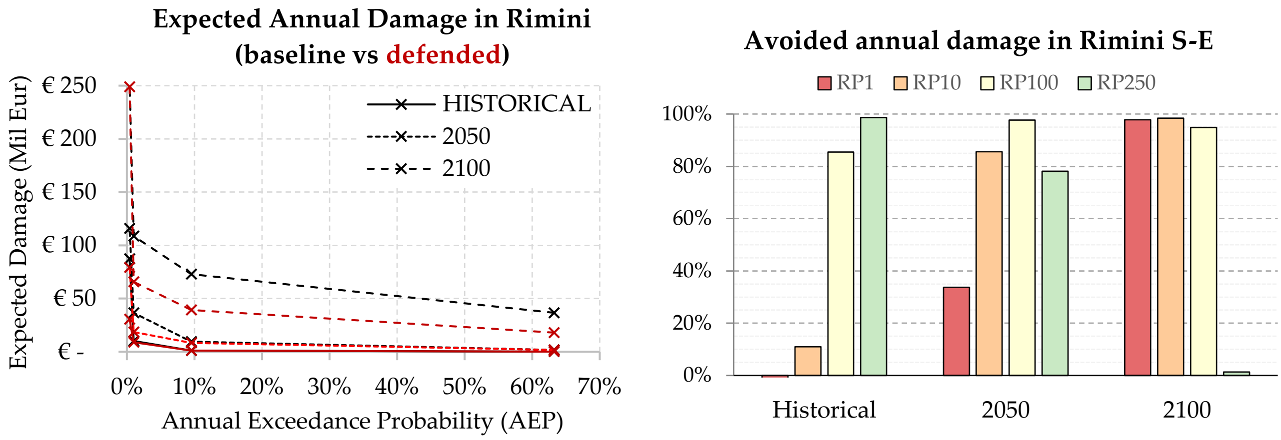

Figure 9. Rimini: Expected Annual Damage (EAD) according to undefended scenario up to 2100, all town considered [left]; EAD reduction in the south-eastern part of the town thanks to hazard mitigation offered by the coastal barrier [right].

In Cesenatico, the average EAD for the undefended scenario grows from around 270 thousand Eur under historical conditions, to 1.7 million Eur in 2050 and almost 26 million Eur in 2100. In our simulations, the designed defence structure (a static barrier with height of 2.8 m along 7.8 km of coast) is able to avoid most of the damage inflicted to residential buildings (Figure **10**, left). The measure becomes less efficient for the most extreme scenarios in 2050 and 2100, when the increase in TWL causes the surmounting of the barrier (Figure **10**, right). This assessment does not account for the impacts over those beach resorts and bathing facilities which are located along the barrier or between the barrier and the sea, and thus are equally exposed in both the baseline and the defended scenario; they would likely represent an additional 7-25% of the baseline damage.

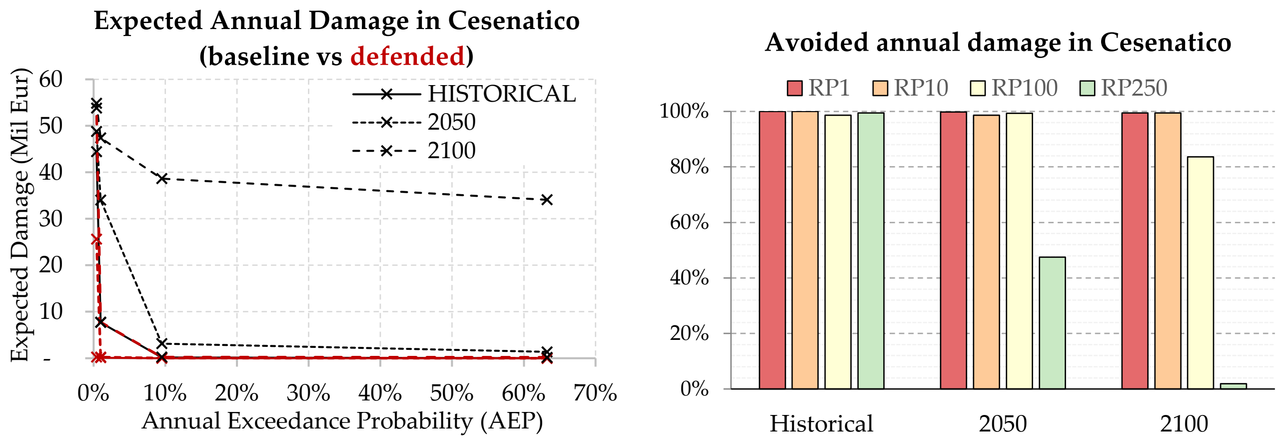

Figure 10. Cesenatico: Expected Annual Damage (EAD) according to undefended scenario up to 2100 [left]; EAD reduction thanks to hazard mitigation offered by the coastal barrier [right].

4.3 Cost-Benefit Analysis

The estimates of avoided direct flood impacts are accounted in a DRR-oriented CBA to evaluate the feasibility of mitigation measures in terms of NPV, BCR and payback period for the two time-horizons (2021-2050: 30 years; and 2021-2100: 80 years). The assessment does not measure the indirect benefits brought in terms of urban renovation, which are the primary focus of the *Parco del Mare* project, measuring, instead, only the direct benefits in terms of direct flood damage reduction. In Figure **11**, the Expected Annual Benefits (EAB) grow at faster rate approaching 2100 in both sites, because of the larger expected damages from more intense, less frequent flood events. The cost of defence implementation is repaid by avoided damage after about 40 years in Cesenatico and after 90 years in Rimini. At 2100, the BCR is 0.9 for Rimini and 1.8 for Cesenatico. These results clearly indicate an overall profitability of the defence structure implementation over the long term for Cesenatico. For the case of the municipality of Rimini, further investigation is required in order to account for the non-DRR benefits of the seafront renovation project. For instance, the potential reduction in indirect losses in terms of capital and labour productivity due to less frequent and less intense flooding events, and the potential increase in tourism and well-being of citizens due to renewed urban landscape, are factors that could be accounted for in a holistic CBA analysis and would likely return a shorter payback period.

In order to better understand the potential benefits of the mitigation measures over different areas of the two municipalities, we compare the results in terms of CBR over a selection of exposed records corresponding to the town higher-density area (i.e. Cesenatico historical center). Table **2** summarizes the metrics of the assessment for different area extent selections. Results do not differ much when comparing the CBA over different areas. In Cesenatico benefits grow proportionally to costs, so that the payback time does not change when considering a section of the town or the whole coastal perimeter.

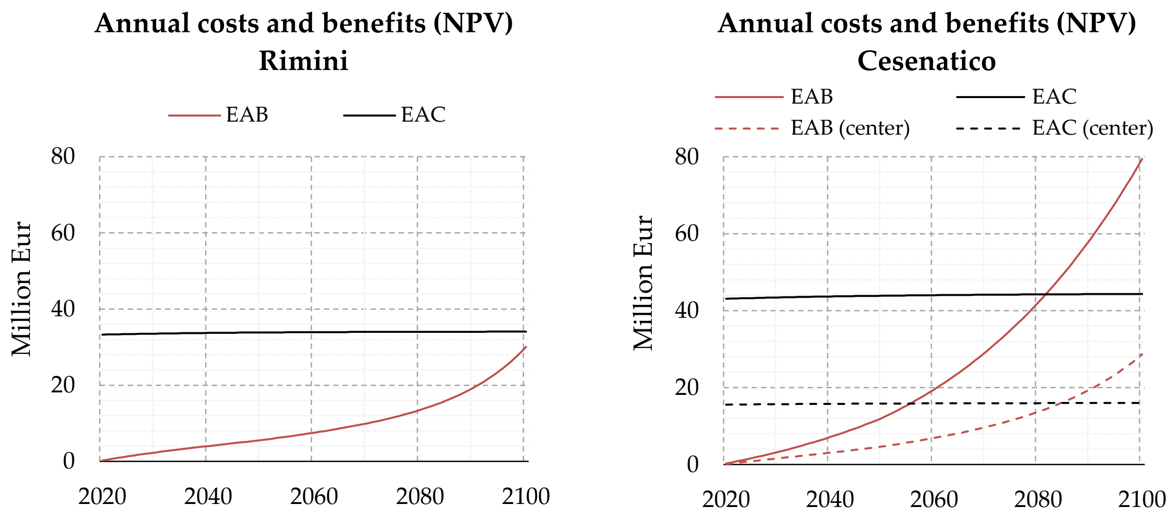

Figure 11. Cumulated flood defence costs and expected benefits at Net Present Value for Rimini (left) and Cesenatico (right).

Table 2. Summary of CBA for planned or designed seaside defence project in Rimini (all town and south section only) and Cesenatico (all town and center only) over a time horizon of 30 and 80 years (2021 to 2050 and 2021 to 2100).

	Rimini				**Cesenatico**			
	All town		*South only*		*All town*		*Center only*	
Metrics	2050	2100	2050	2100	2050	2100	2050	2100
Baseline EAD [M EUR]	2.8	32	0.5	14.6	1.7	25.9	0.5	12.4
Defended EAD [M EUR]	2.4	17	0.1	0.9	0.1	0.4	0.1	0.4
Expected Annual Benefits [M EUR]	0.3	15	0.4	13.7	1.6	25.5	0.4	11.9
Sum of EAB (discounted) [M EUR]	5.6	30	4.1	27.8	12.0	79.4	4.7	28.6
Sum of EAC (discounted) [M EUR]	33.8	34.0	33.8	34.0	43.8	44.3	15.8	16.0
Net Present Value [M EUR]	-28.3	-4.0	-29.8	-6.3	-31.8	35.1	-11.24	12.6
Benefit-Cost ratio [-]	0.16	0.88	0.12	0.81	0.28	1.79	0.30	1.79

5. Conclusion

In this study we addressed coastal inundation risk scenarios over two coastal towns located along the North Adriatic coastal plain of Italy, which is projected to become increasingly exposed to ESL events due to changes in MSL induced by SLR and local subsidence phenomena. Both locations are expected to suffer increasing economic losses from these events, unless effective coastal adaptation measures are put in place. To understand the upcoming impacts and the potential benefits of designed coastal projects, we run a CBA comparing the baseline and the defended scenario in terms of flood losses over residential buildings, which represent the largest share of exposed buildings' footprints (93%). The defended scenario accounts for the effect of a coastal barriers based on the design of *Parco del Mare*, an urban renovation project under construction in Rimini. The same type of defence structure is envisaged along the coastal perimeter of the nearby town of Cesenatico. First, we characterised reference ESL events in terms of frequency and intensity based on local historical observations; then, we projected ESL scenarios to 2050 and 2100, accounting for the combined effect of SLR and subsidence rates on the TWL, as obtained from existing local studies. We produced flood hazard maps estimating maximum flood extent and water depth using a high-resolution hydrodynamic model able to replicate the physics of the inundation process. The hazard maps were fed to a locally-calibrated damage model in order to calculate the expected annual damage for both baseline and defended scenarios. An increase in damage is expected for both urban areas from 2021 to 2100: in Cesenatico the EAD grows by a factor 96, in Rimini by a factor 49.

The results obtained from the CBA on both locations show growing profitability of present project investment over time, associated with the increase of damage triggered by intense ESL events: the EAD under the baseline hypothesis is expected to increase by 3.5-fold in 2050, up to 10-fold in 2100. The benefits brought by the coastal defence project become much larger in the second half of the century: the EAB grows 6.1-fold in Rimini, 6.5-fold in Cesenatico, from 2050 to 2100. Avoided losses are expected to match the project implementation costs after about 40 years in Cesenatico and 90 years in Rimini. Benefits are found to increase proportionally to costs; the payback period in Cesenatico is the same considering either an investment on the protection of the whole town or only part of it. Further assessments of these renovation projects should look to measure the indirect and spill-over effects over the local economy brought by the project, possibly accounting also for the intangible benefits and scenarios of exposure change. The results are calculated in relation to emission scenario RCP 4.5; compared to RCP 8.5 at 2050, the difference in SLR contribution is negligible (~0.05 m), while at 2100, the difference between the two emission scenarios is larger (around 0.2 m), thus additional scenario analysis is suggested in future research.

Data availability

Mattia Amadio, & Arthur H. Essenfelder. (2021). Coastal flood inundation scenarios over Cesenatico and Rimini: hazard and risk for Business as Usual and Defended options [Data set]. Hosted by Zenodo: https://zenodo.org/record/4783443

Authors contribution

MA, AHE and SB conceptualized the study and designed the experiments. AHE carried out the coastal hazard modelling. SR advised the model setup and calculation. SB and PM provided required data and expertise about the case study areas. MA performed the economic risk modelling and wrote the manuscript. SM supported the CBA calculations. JM and SB managed the funding acquisition and project supervision. All co-authors have reviewed the manuscript.

Acknowledgment

The research leading to this paper received funding through the projects CLARA (EU's Horizon 2020 research and innovation programme under grant agreement 730482), SAFERPLACES (Climate-KIC innovation partnership) and EUCP – European Climate Prediction system under grant agreement 776613. We want to thank Luisa Perini for her kind support.

References

Amadio M, Scorzini AR, Carisi F, et al (2019) Testing empirical and synthetic flood damage models: the case of Italy. Nat Hazards Earth Syst Sci 19:661–678 . doi: 10.5194/nhess-19-661-2019

Antonioli F, Anzidei M, Amorosi A, et al (2017) Sea-level rise and potential drowning of the Italian coastal plains: Flooding risk scenarios for 2100. Quat Sci Rev 158:29–43 . doi: 10.1016/j.quascirev.2016.12.021

Armaroli C, Ciavola P, Perini L, et al (2012) Critical storm thresholds for significant morphological changes and damage along the Emilia-Romagna coastline, Italy. Geomorphology 143–144:34–51 . doi: 10.1016/j.geomorph.2011.09.006

Armaroli C, Duo E (2018) Validation of the coastal storm risk assessment framework along the Emilia-Romagna coast. Coast Eng 134:159–167 . doi: 10.1016/j.coastaleng.2017.08.014

ARPAE (2019) Relazione tecnica mappe della pericolosità e del rischio di alluvioni in ambito costiero

Boardman AE, Greenberg DH, Vining AR, Weimer DL (2018) Cost-Benefit Analysis. Cambridge University Press

Bonaduce A, Pinardi N, Oddo P, et al (2016) Sea-level variability in the Mediterranean Sea from altimetry and tide gauges. Clim Dyn 47:2851–2866 . doi: 10.1007/s00382-016-3001-2

Boon JD (2004) Secrets of the Tide: Tide and Tidal Current Analysis and Predictions, Storm Surges and Sea Level Trends. Elsevier Inc.

Bos F, Zwaneveld P (2017) Cost-Benefit Analysis for Flood Risk Management and Water Governance in the Netherlands: An Overview of One Century. SSRN Electron J. doi: 10.2139/ssrn.3023983

Bouwer LM (2011) Have disaster losses increased due to anthropogenic climate change? Bull Am Meteorol Soc. doi: 10.1175/2010BAMS3092.1

Carbognin L, Teatini P, Tomasin A, Tosi L (2010) Global change and relative sea level rise at Venice: What impact in term of flooding. Clim Dyn 35:1055–1063 . doi: 10.1007/s00382-009-0617-5

Carbognin L, Teatini P, Tosi L (2009) The impact of relative sea level rise on the Northern Adriatic Sea coast, Italy. WIT Trans Ecol Environ 127:137–148 . doi: 10.2495/RAV090121

Carminati E, Martinelli G (2002) Subsidence rates in the Po Plain, northern Italy: the relative impact of natural and anthropogenic causation. Eng Geol 66:241–255 . doi: 10.1016/S0013-7952(02)00031-5

Church JA, White NJ (2011) Sea-Level Rise from the Late 19th to the Early 21st Century. Surv Geophys 32:585–602 . doi: 10.1007/s10712-011-9119-1

Ciavola P, Coco G (eds) (2017) Coastal storms: processes and impacts. Wiley-Blackwell

Comune di Rimini (2018) Parco del Mare Sud - Strategia per la rigenerazione urbana

Comune di Rimini (2019a) Deliberazione originale di giunta comunale N. 99 del 11/04/2019

Comune di Rimini (2019b) Deliberazione originale di giunta comunale N. 118 del 02/05/2019

Comune di Rimini (2020) Deliberazione originale di giunta comunale N. 128 del 26/05/2020

Comune di Rimini (2021a) Deliberazione originale di giunta comunale N. 19 del 19/01/2021

Comune di Rimini (2021b) Deliberazione originale di giunta comunale N. 20 del 19/01/2021

CRESME (2014) Definizione dei costi di (ri)costruzione nell'edilizia

Familkhalili R, Talke SA, Jay DA (2020) Tide-Storm Surge Interactions in Highly Altered Estuaries: How Channel Deepening Increases Surge Vulnerability. J Geophys Res Ocean 125:e2019JC015286 . doi: 10.1029/2019JC015286

Froehlich DC (2002) IMPACT Project Field Tests 1 and 2: "Blind" Simulation. 1–18

Fuhrmann CM, Wood KM, Rodgers JC (2019) Assessment of storm surge and structural damage on San Salvador Island, Bahamas, associated with Hurricane Joaquin (2015). Nat Hazards 99:913–930 . doi: 10.1007/s11069-019-03782-2

Gambolati G, Giunta G, Putti M, et al (1998) Coastal Evolution of the Upper Adriatic Sea due to Sea Level Rise and Natural and Anthropic Land Subsidence. 1–34 . doi: 10.1007/978-94-011-5147-4

Garnier E, Ciavola P, Spencer T, et al (2018) Historical analysis of storm events: Case studies in France, England, Portugal and Italy. Coast Eng 134:10–23 . doi: 10.1016/j.coastaleng.2017.06.014

Geofabrik GmbH (2018) OpenStreetMap data extracts

Hallegatte S, Green C, Nicholls RJ, Corfee-Morlot J (2013) Future flood losses in major coastal cities. Nat Clim Chang. doi: 10.1038/nclimate1979

Hinkel J, Lincke D, Vafeidis AT, et al (2014) Coastal flood damage and adaptation costs under 21st century sea-level rise. Proc Natl Acad Sci. doi: 10.1073/pnas.1222469111

Huizinga J, Moel H De, Szewczyk W (2017) Global flood depth-damage functions : Methodology and the Database with Guidelines

IPCC (2019) IPCC Special Report on the Ocean and Cryosphere in a Changing Climate

ISPRA (2012) Mare e ambiente costiero. Temat Primo Piano - Annu dei dati Ambient 2011 259–322

ISTAT (2011) 15° censimento della populazione e delle abitazioni

Jongman B, Kreibich H, Apel H, et al (2012a) Comparative flood damage model assessment: towards a European approach. Nat Hazards Earth Syst Sci 12:3733–3752

Jongman B, Ward PJ, Aerts JCJH (2012b) Global exposure to river and coastal flooding: Long term trends and changes. Glob Environ Chang. doi: 10.1016/j.gloenvcha.2012.07.004

Jonkman SN, Brinkhuis-Jak M, Kok M (2004) Cost benefit analysis and flood damage mitigation in the Netherlands. Heron 49:95–111

Kain CL, Lewarn B, Rigby EH, Mazengarb C (2020) Tsunami Inundation and Maritime Hazard Modelling for a Maximum Credible Tsunami Scenario in Southeast Tasmania, Australia. Pure Appl Geophys 177:1549–1568 . doi: 10.1007/s00024-019-02384-0

Kemp AC, Horton BP, Donnelly JP, et al (2011) Climate related sea-level variations over the past two millennia. Proc Natl Acad Sci U S A 108:11017–11022 . doi: 10.1073/pnas.1015619108

Kind JM (2014) Economically efficient flood protection standards for the Netherlands. J Flood Risk Manag 7:103–117 . doi: 10.1111/jfr3.12026

Kirezci E, Young IR, Ranasinghe R, et al (2020) Projections of global-scale extreme sea levels and resulting episodic coastal flooding over the 21st Century. Sci Rep 10:1–12 . doi: 10.1038/s41598-020-67736-6

Lambeck K, Antonioli F, Anzidei M, et al (2011) Sea level change along the Italian coast during the Holocene and projections for the future. Quat Int 232:250–257 . doi: 10.1016/j.quaint.2010.04.026

Lambeck K, Purcell A (2005) Sea-level change in the Mediterranean Sea since the LGM: Model predictions for tectonically stable areas. In: Quaternary Science Reviews. Pergamon, pp 1969–1988

Lionello P (2012) The climate of the Venetian and North Adriatic region: Variability, trends and future change. Phys Chem Earth 40–41:1–8 . doi: 10.1016/j.pce.2012.02.002

Lionello P, Barriopedro D, Ferrarin C, et al (2020) Extremes floods of Venice: characteristics, dynamics, past and future evolution. Nat Hazards Earth Syst Sci 1–34 . doi: 10.5194/nhess-2020-359

Lionello P, Conte D, Marzo L, Scarascia L (2017) The contrasting effect of increasing mean sea level and decreasing storminess on the maximum water level during storms along the coast of the Mediterranean Sea in the mid 21st century. Glob Planet Change 151:80–91 . doi: 10.1016/j.gloplacha.2016.06.012

Lowe J (2008) Intergenerational wealth transfers and social discounting: Supplementary Green Book guidance. HM Treasury, London 3–6

Lowe J, Gregory J, Flather R (2001) Changes in the occurrence of storm surges around the United Kingdom under a future climate scenario using a dynamic storm surge model driven by the Hadley Centre climate models. Clim Dyn 18:179–188

Marsico A, Lisco S, Lo Presti V, et al (2017) Flooding scenario for four italian coastal plains using three relative sea level rise models. J Maps 13:961–967 . doi: 10.1080/17445647.2017.1415989

Masina M, Lamberti A, Archetti R (2015) Coastal flooding: A copula based approach for estimating the joint probability of water levels and waves. Coast Eng 97:37–52 . doi: 10.1016/j.coastaleng.2014.12.010

McGranahan G, Balk D, Anderson B (2007) The rising tide: Assessing the risks of climate change and human settlements in low elevation coastal zones. Environ Urban. doi: 10.1177/0956247807076960

McInnes KL, Walsh KJE, Hubbert GD, Beer T (2003) Impact of sea-level rise and storm surges in a coastal community. Nat Hazards 30:187–207 . doi: 10.1023/A:1026118417752

Mechler R (2016) Reviewing estimates of the economic efficiency of disaster risk management: opportunities and limitations of using risk-based cost–benefit analysis. Nat Hazards 81:2121–2147 . doi: 10.1007/s11069-016-2170-y

Melet A, Almar R, Hemer M, et al (2020) Contribution of Wave Setup to Projected Coastal Sea Level Changes. J Geophys Res Ocean 125:e2020JC016078 . doi: 10.1029/2020JC016078

Meli M, Olivieri M, Romagnoli C (2021) Sea-level change along the emilia-romagna coast from tide gauge and satellite altimetry. Remote Sens 13:1–26 . doi: 10.3390/rs13010097

Meyssignac B, Cazenave A (2012) Sea level: A review of present-day and recent-past changes and variability. J. Geodyn. 58:96–109

Mitchum GT, Nerem RS, Merrifield MA, Gehrels WR (2010) Modern Sea-Level-Change Estimates. In:

Understanding Sea-Level Rise and Variability. Wiley-Blackwell, Oxford, UK, pp 122–142

Muis S, Verlaan M, Winsemius HC, et al (2016) A global reanalysis of storm surges and extreme sea levels. Nat Commun 7:1–11 . doi: 10.1038/ncomms11969

Nicholls RJ, Cazenave A (2010) Sea-level rise and its impact on coastal zones. Science (80-) 328:1517–1520 . doi: 10.1126/science.1185782

Olsen AS, Zhou Q, Linde JJ, Arnbjerg-Nielsen K (2015) Comparing methods of calculating expected annual damage in urban pluvial flood risk assessments. Water (Switzerland) 7:255–270 . doi: 10.3390/w7010255

Peltier WR (2004) Global Glacial Isostasy and the surface of the ice-age Earth: the ICE-5G (VM2) Model and GRACE. Annu Rev Earth Planet Sci 32:111–149 . doi: 10.1146/annurev.earth.32.082503.144359

Peltier WR, Argus DF, Drummond R (2015) Space geodesy constrains ice age terminal deglaciation: The global ICE-6G_C (VM5a) model. J Geophys Res Solid Earth 120:450–487 . doi: 10.1002/2014JB011176

Perini L, Calabrese L, Deserti M, et al (2011) Le mareggiate e gli impatti sulla costa in Emilia-Romagna 1946-2010

Perini L, Calabrese L, Lorito S, Luciani P (2015) Il rischio da mareggiata in Emilia-Romagna: l'evento del 5-6 Febbraio 2015. Geol 53:8–17

Perini L, Calabrese L, Luciani P, et al (2017) Sea-level rise along the Emilia-Romagna coast (Northern Italy) in 2100: Scenarios and impacts. Nat Hazards Earth Syst Sci 17:2271–2287 . doi: 10.5194/nhess-17-2271-2017

Perini L, Calabrese L, Salerno G, et al (2016) Evaluation of coastal vulnerability to flooding: Comparison of two different methodologies adopted by the Emilia-Romagna region (Italy). Nat Hazards Earth Syst Sci 16:181–194 . doi: 10.5194/nhess-16-181-2016

Perini L, Calabrese L, Salerno G, Luciani P (2012) Mapping of flood risk in Emilia-Romagna coastal areas. Rend Online Soc Geol Ital 21:501–502 . doi: 10.13140/2.1.1703.7766

Polcari M, Albano M, Montuori A, et al (2018) InSAR monitoring of Italian coastline revealing natural and anthropogenic ground deformation phenomena and future perspectives. Sustain 10:4–7 . doi: 10.3390/su10093152

Price R (2018) Cost-effectiveness of disaster risk reduction and adaptation to climate change. 1–21

Roberts S (2020) ANUGA - Open source hydrodynamic / hydraulic modelling

Roberts S, Nielsen O, Gray D, Sexton J (2015) ANUGA User Manual

Scarascia L, Lionello P (2013) Global and regional factors contributing to the past and future sea level rise in the Northern Adriatic Sea. Glob Planet Change 106:51–63 . doi: 10.1016/j.gloplacha.2013.03.004

Solari L, Del Soldato M, Bianchini S, et al (2018) From ERS 1/2 to Sentinel-1: Subsidence Monitoring in Italy in the Last Two Decades. Front Earth Sci 6: . doi: 10.3389/feart.2018.00149

Stocker TF, Dahe Q, Plattner G-K, et al (2013) Technical Summary. In: Stocker TF, Qin D, Plattner G-K, et al. (eds) Climate Change 2013: The Physical Science Basis. Contribution of Working Group I to the Fifth Assessment Report of the Intergovernmental Panel on Climate Change. Cambridge University Press, Cambridge, United Kingdom and New York, NY, USA., pp 33–115

Syvitski JPM, Kettner AJ, Overeem I, et al (2009) Sinking deltas due to human activities. Nat Geosci. doi: 10.1038/ngeo629

Teatini P, Ferronato M, Gambolati G, et al (2005) A century of land subsidence in Ravenna, Italy. Environ Geol 47:831–846 . doi: 10.1007/s00254-004-1215-9

Teatini P, Ferronato M, Gambolati G, Gonella M (2006) Groundwater pumping and land subsidence in the Emilia-Romagna coastland, Italy: Modeling the past occurrence and the future trend. Water Resour Res 42: . doi: 10.1029/2005WR004242

Tsimplis MN, Marcos M, Somot S (2008) 21st century Mediterranean sea level rise: Steric and atmospheric pressure contributions from a regional model. Glob Planet Change 63:105–111 . doi: 10.1016/j.gloplacha.2007.09.006

Tsimplis MN, Raicich F, Fenoglio-Marc L, et al (2012) Recent developments in understanding sea level rise at the Adriatic coasts. Phys Chem Earth 40–41:59–71 . doi: 10.1016/j.pce.2009.11.007

Tsimplis MN, Rixen M (2002) Sea level in the Mediterranean Sea: The contribution of temperature and salinity changes. Geophys Res Lett 29:51-1-51–4 . doi: 10.1029/2002gl015870

Umgiesser G, Bajo M, Ferrarin C, et al (2020) The prediction of floods in Venice: methods, models and uncertainty. Nat Hazards Earth Syst Sci 1–47 . doi: 10.5194/nhess-2020-361

Vousdoukas MI, Mentaschi L, Feyen L, Voukouvalas E (2017) Extreme sea levels on the rise along Europe's coasts. Earth's Futur 5:1–20 . doi: 10.1002/eft2.192

Vousdoukas MI, Mentaschi L, Voukouvalas E, et al (2018) Global probabilistic projections of extreme sea levels show intensification of coastal flood hazard. Nat Commun 9:1–12 . doi: 10.1038/s41467-018-04692-w

Wöppelmann G, Marcos M (2012) Coastal sea level rise in southern Europe and the nonclimate contribution of vertical land motion. J Geophys Res Ocean 117: . doi: 10.1029/2011JC007469

Zanchettin D, Bruni S, Raicich F, et al (2020) Review article: Sea-level rise in Venice: historic and future trends. Nat Hazards Earth Syst Sci Discuss 1–56 . doi: 10.5194/nhess-2020-351

Zanchettin D, Traverso P, Tomasino M (2007) Observations on future sea level changes in the Venice lagoon. Hydrobiologia. doi: 10.1007/s10750-006-0416-5

Annex 1

RP 1 year

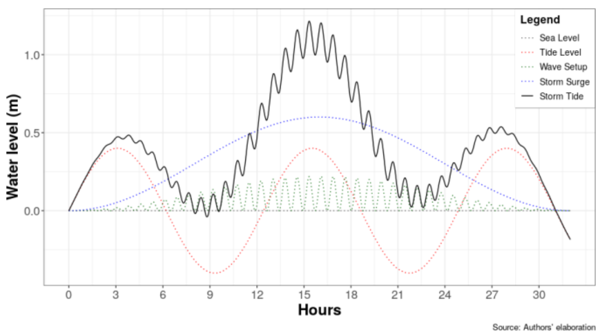

RP 10 years

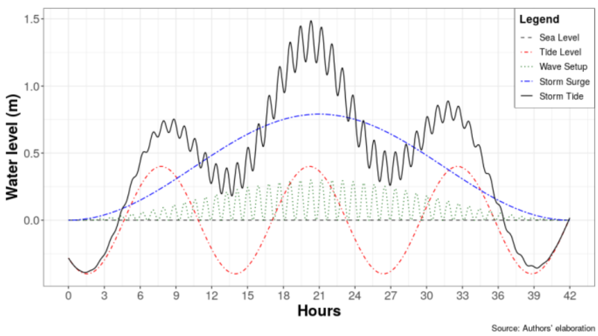

RP 100 years

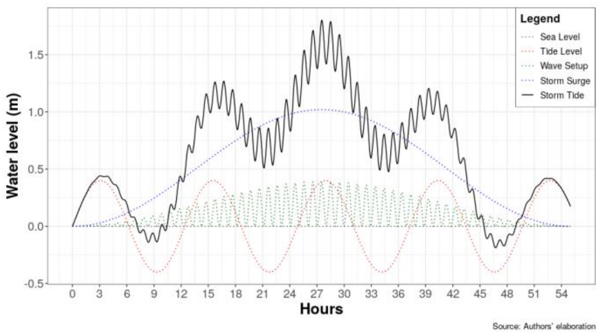

RP 250 years

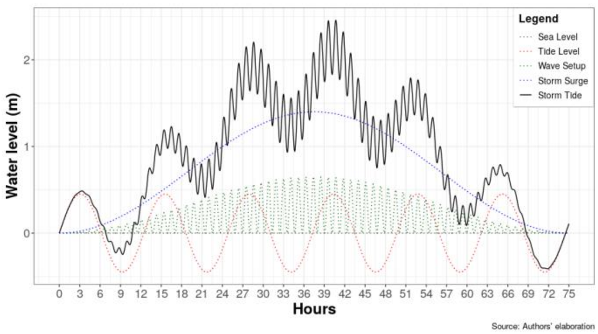

Figure A1. Dynamic boundary conditions for simulating theoretical storm surge events in ANUGA. Total Water Level (black) as a sum of tide (red), storm surge (blue) and wave setup (green) for all simulated ESL scenarios (Return Period of once-in-1, 10, 100 and 250 years).

Annex 2

A sensitivity analysis is carried out on the discount rate. Figure A2 below shows how the NPV changes with discount rate *r* ranging from 1.5% to 5.5% (2020 to 2050) and 1% to 5% (2050-2100).

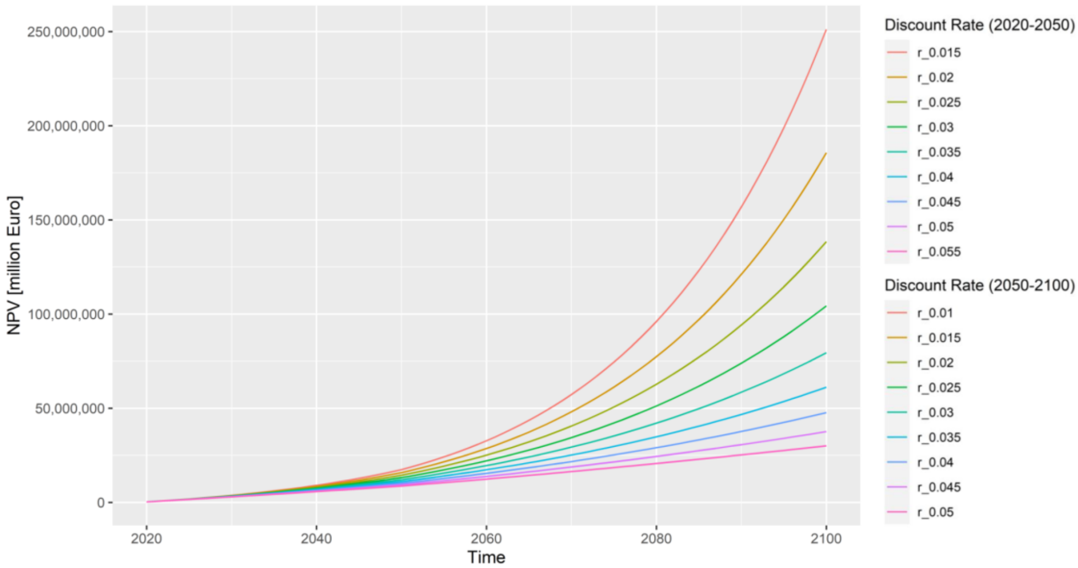

Figure A2. Sensitivity analysis of NPV using a variable discount rate.